Outage Probability Analysis of UAV-Aided Millimeter Wave Communication Network

A Project Report

Submitted by

BATHILI NAVEEN KUMAR

in partial fulfillment of the requirements

for the award of the degree of

MASTER OF TECHNOLOGY

Department Of Electrical Engineering

INDIAN INSTITUTE OF TECHNOLOGY MADRAS

JUNE 2021

DEPARTMENT OF ELECTRICAL ENGINEERING

INDIAN INSTITUTE OF TECHNOLOGY MADRAS

2021

THESIS CERTIFICATE

This is to certify that this thesis titled **"Outage Probability Analysis of UAV-Aided Millimeter Wave communication network "** submitted by **Bathili Naveen Kumar (EE19M089)** to the Indian Institute of Technology Madras, for the award of the degree of **Masters of Technology** is a bonafide record of the research work done by him under my supervision. The contents of this thesis, in whole or in parts, have not been submitted to any other Institute or University for the award of any degree or diploma.

Dr. Sheetal Kalyani
Project Guide,
Associate Professor,
Department of Electrical Engineering,
IIT Madras, 600036.
Chennai, June, 2021

ACKNOWLEDGMENTS

First and foremost, I would like to express my deepest gratitude to my guide, **Dr. Sheetal Kalyani**, Associate Professor, Department of Electrical Engineering, IIT Madras, for providing me an opportunity to work under her. I want to express my deepest appreciation for her patience, valuable feedback, suggestions, and motivations.

I convey my sincere gratitude to Ph.D. guys, namely Muralikrishnan and Athira, IIT Madras, for all suggestions and support during the entire course of the project. Throughout the project, they offered immense help and provided valuable advice that helped me complete this project.

I want to extend my appreciation to all my Professors whose courses helped me improve my knowledge and my friends for their help and support in completing my project successfully.

ABSTRACT

Unmanned aerial vehicles (UAV) are potential candidates for mobile aerial base stations (BS's) which can aid in the deployment of reliable millimetre wave communication systems. Moreover they can support long transmission distances and extensive coverage range. In this letter, we derive simple approximations for evaluating the outage probability (OP) of the ground users of a system with an UAV BS equipped with a uniform planar array (UPA) of antennas. We use the method of moment matching to derive approximate expressions for the cumulative distribution function (CDF) of the received signal to interference plus noise ratio (SINR). Using this CDF, we derive the OP, and analyze the different terms in OP with respect to variations in certain system parameters. Furthermore, we present simulation results to corroborate the utility of the results proposed.

Contents

List of Tables

List of Figures

ABBREVIATIONS

UAV	Unmanned Aerial Vehicle
UPA	Uniform Planar Array
LOS	Line Of Sight
NLOS	Non-Line of Sight
OP	Outage Probability
SINR	Signal to Interference plus Noise Ratio
PDF	Probability Density Function
CDF	Cumulative Distribution Function

Chapter 1

Introduction

1.1 Introduction to UAV-aided mmWave network

One promising approach to augment the performance of cellular communication is by introducing air-based platforms such as an UAV's or a high-altitude platforms (HAP) for deploying base stations or relays. There have been extensive surveys on the design, channel modeling, and security of UAV based cellular communication. One of the major challenges of using UAV's is to have realistic air to ground (AG) propagation model and the design of large and small scale fading models for different environments and scenarios [1]. New regulations are being developed to manage the commercial use of UAV's in cellular communication to overcome security concerns, interference issues [2] and other challenge's. The performance of UAV-aided cellular networks mostly depend on the altitude of the UAV and this unique ability can be used to serve efficiently in different environments [3].

The authors of [4] study the prospects of deploying UAV's as flying base stations

to provide wireless communication to a given area, to enhance coverage and study the trade-off between coverage and delay in UAV aided systems. To optimize the network for multiple destinations, the authors of [5] proposes an algorithm to find the optimum altitude of the UAV for maximum coverage region by guaranteeing a minimum outage performance. The authors of [6] analyses the downlink coverage of UAV aided systems to reveal several use-full trends in coverage probability as a function of the UAV height. To obtain the optimum system parameters in terms of the drones antenna beamwidth, density and altitude, the authors of [7] proposes an algorithm for coverage maximization. The authors of [8] discusses the coverage probability analysis for the low altitude UAV network in urban environments. A critical cornerstone of the next-generation communication systems is the potential exploitation of the unused spectrum of mmwave carrier frequencies for information transmission. In this direction, the authors of [9–14] have investigated the challenges of mmwave based A2G and air-to-air (A2A) communications. The applicability of the two-ray propagation model in different scenarios employing UAVs was explored in [9]. The pros and cons of UAV-BS in complementing the mmwave back-haul was demonstrated in [10]. The concept of mmwave A2A networks was first explored by Cuvelier and Heath [12], while mmwave based HAP's in terrestrial transmissions were studied in [13, 14]. The UAV is mounted with planner arrays to improve the performance of beam-forming and their use as adaptive multi-beam antennas is discussed in [15]. Experiments have shown that beam-forming can improve the performance in different applications like CDMA wireless communication systems. The authors of [16] used a null steering beam-forming algorithm to suppress co-channel interference. In the mmwave communication systems, beam-forming is also used to improve the spectral efficiency without improving the complexity when the beam pointing is unstable,this was demonstrated in [17, 18]. Similar to the system model discussed in [15], the use of a UPA mounted on a UAV to improve the beam gain in mmwave beamforming is discussed in [19]. To achieve flexible beam coverage for any type of target area in mmwave UAV communications, the authors of [20] used 3D-beam forming. Reinforcement learning approach is proposed by authors

of [21] to improve the maximal coverage while taking into account the human body blockage effects.

The rest of the paper is structured as follows. In Section II, the proposed system model is discussed in detail. In Section III, approximate expressions are derived for the CDF of SINR LoS, NLoS using moment-matching approximation. We derive the OP, and analyze the different terms in OP with respect to the variations in specific system parameters in Section IV. In Section V, our simulation results are presented, and in Section VI, conclusion and some future works are provided.

Chapter 2

System Model

In this chapter, we discuss the system model for the analysis of the UAV aided communication system studied in this thesis.

2.1 Geometric Structure

Consider a UAV equipped with a UPA of dimensions $M \times M$ positioned at the origin of the coordinate system. Let z_u be the height of UAV from the ground [20]. Assume the x-axis is parallel to an edge of the UPA, z-axis is perpendicular to the ground. The N single antenna users are at $(x_i, y_i, -z_u)$ $i = 1, ..., N$. Let (θ_i^z, θ_i^a) represent the zenith and azimuth angle pair for the i^{th} user, which are:

$$\theta_i^z = \tan^{-1}\left(\frac{\sqrt{x_i^2 + y_i^2}}{-z_u}\right), \quad i = 1, ..., N \tag{2.1.1}$$

Notation	Environment	a_0	b_0	η_L(dB)	η_{NL}(dB)
En1	Urban	9.61	0.16	1.0	20
En2	Dense Urban	12.08	0.11	1.6	23
En3	High-rise Urban	27.23	0.08	2.3	34

Table 2.1: Environment parameters

and

$$\theta_i^a = \tan^{-1}\left(\frac{y_i}{x_i}\right), \quad i = 1, ..., N. \tag{2.1.2}$$

For $i = 1, .., N$, let $\mathbf{e}_i$ be the $M^2 \times 1$ vector representation of the ith user's steering vector with respect to each of the components of the planar array. The three-dimensional Cartesian co-ordinates of the (m, n)th component of the planar array are represented by $(x_m, y_n, 0)$, where $x_m = \left[-\frac{M-1}{2} + (m-1)\right]\frac{\lambda}{2}$ and $y_n = \left[-\frac{M-1}{2} + (n-1)\right]\frac{\lambda}{2}$, for $m = 1, ..., M$ and $n = 1, ..., M$. Note that the inter-elemental spacing is $\lambda/2$, where λ is the wavelength of the carrier. Thus the entry of $\mathbf{e}_i$, which corresponds to the position of the user with respect to the (m, n)th element of the planar array, is given by $\exp\left[j\frac{2\pi}{\lambda}\left(x_m\psi_i^x + y_n\psi_i^y\right)\right]$, where we have

$$\psi_i^x = \sin\theta_i^z \cos\theta_i^a, \tag{2.1.3}$$

and

$$\psi_i^y = \sin\theta_i^z \sin\theta_i^a, \tag{2.1.4}$$

while θ_i^z and θ_i^a are defined in (2.1.1) and (2.1.2), respectively, which are functions of the user location.

2.2 Pathloss and Pathloss exponents

At the users, two different instantaneous SINR is possible depending on the probability of Los [22], which is in turn dependent on the zenith angle and the type of channel setting (urban, dense urban, high-rise).

$$P_{Los}\left(\theta_i^z\right) = \frac{1}{1 + a_0 \exp\left(-b_0\left[\left(\frac{\pi}{2} - \theta_i^z - a_0\right]\right)\right)}, i = 1, ..., N \tag{2.2.1}$$

Similarly, probability of a non-line-of-sight path is given in (2.2.2)

$$P_{NLos}\left(\theta_i^z\right) = 1 - P_{LoS}\left(\theta_i^z\right), i = 1, ..., N \tag{2.2.2}$$

The relationship between the path-loss exponent and zenith angle is given in (2.2.3)

$$\alpha_i = a_1 P_{LoS}\left(\theta_i^z\right) + b_1, \tag{2.2.3}$$

Where, $a_1 = \alpha_{(\pi/2)} - \alpha_0$ and $b_1 = \alpha_0$, take $\alpha_{(\pi/2)} = 2$ and $\alpha_0 = 4$. The path loss of the Los and Nlos channel links are given by (2.2.4) and (2.2.5) respectively.

$$\beta_i^L = \eta_L \left(z_u^2 + r_i^2\right)^{\frac{\alpha_i}{2}}, \tag{2.2.4}$$

$$\beta_i^{NL} = \eta_{NL} \left(z_u^2 + r_i^2\right)^{\frac{\alpha_i}{2}}, \tag{2.2.5}$$

Where, z_u is the height of the UAV from ground and for the i-th user $r_i = \sqrt{x_i^2 + y_i^2}$ and the Rician factor (K_i) is given in (2.2.6).

$$K_i = a_2 e^{b_2\left(\frac{\pi}{2} - \theta_i^z\right)}, \tag{2.2.6}$$

Where, $a_2 = K_0, b_2 = \frac{2}{\pi}\log\left(\frac{K\pi}{2K_0}\right)$. Let's take $K_0 = 2$ dB and $K(\frac{\pi}{2}) = 5$ dB. For the Los path, K is the Rician factor, and $K = 0$ for the Nlos path. The Rician fading

channel the UAV and the i-th user is represented by:

$$\mathbf{h}_{i,Ric} = \sqrt{\frac{K_i}{1+K_i}}\mathbf{e}_i + \sqrt{\frac{1}{1+K_i}}\mathbf{h}_i, \tag{2.2.7}$$

Where, K_i is the Rician factor, $\mathbf{h}_i$ is the Nlos component, and $\mathbf{e}_i$ is the steering vector.

2.3 SINR

The symbol received by the i-th user if Los is

$$y_i = \sqrt{\frac{P_t}{\beta_i^L}}\mathbf{h}_{i,Ric}^H\mathbf{e}_i x_i + \sqrt{\frac{P_t}{\beta_i^L}}\sum_{j=1,j\neq i}^{N}\mathbf{h}_{i,Ric}^H\mathbf{e}_j x_j + n, \tag{2.3.1}$$

and if Nlos is

$$y_i = \sqrt{\frac{P_t}{\beta_i^{NL}}}\mathbf{h}_i^H\mathbf{e}_i x_i + \sqrt{\frac{P_t}{\beta_i^{NL}}}\sum_{j=1,j\neq i}^{N}\mathbf{h}_i^H\mathbf{e}_j x_j + n, \tag{2.3.2}$$

Where, n represents the complex Gaussian noise having the power of $\sigma^2 = kTBN_F$, with $k = 1.374 \times 10^{-23}$ being Boltzmann's constant, T the temperature in Kelvins, B the bandwidth, and N_F the noise figure of the receiver. Thus, the SINR of the i-th user, for the Los and Nlos path are given by (2.3.3) and (2.3.4) respectively.

$$\gamma_L^i = \frac{\left|\boldsymbol{h}_{i,Ric}^H\mathbf{e}_i\right|^2}{\sum_{j\neq i}^{N}\left|\boldsymbol{h}_{i,Ric}^H\mathbf{e}_j\right|^2 + \frac{\beta_i^L}{P_t}\sigma^2}, \tag{2.3.3}$$

and

$$\gamma_{NL}^i = \frac{\left|\boldsymbol{h}_i^H\mathbf{e}_i\right|^2}{\sum_{j\neq i}^{N}\left|\boldsymbol{h}_i^H\mathbf{e}_j\right|^2 + \frac{\beta_i^{NL}}{P_t}\sigma^2}. \tag{2.3.4}$$

Where, P_t is the transmit power, σ^2 represents the noise power, $\boldsymbol{e}_i$ and $\boldsymbol{e}_j$ are the steering vectors for i-th and j-th users respectively.

Chapter 3

Derivation of the CDF of SINR

In this chapter, we derive approximate expressions for the distributions of γ_L^i and γ_{NL}^i.

3.1 SINR LOS

Lemma 3.1.1. *The distribution of γ_L^i can be approximated as*

$$F_{\gamma_L^i}(x) = \frac{B\left[\frac{\mathrm{x}}{\mathrm{x}+\frac{\theta_{L,i,1}}{\theta_{L,i,2}}}, k_{L,i,1}, k_{L,i,2}\right]}{B\left[k_{L,i,1}, k_{L,i,2}\right]}; \quad \mathrm{x} > 0, \tag{3.1.1}$$

Where, $\theta_{L,i,1}$, $k_{L,i,1}$, $\theta_{L,i,2}$ and $k_{L,i,2}$ can be evaluated using (3.1.7) and (3.1.9). Here, $B[.,.,.]$ is the incomplete beta function evaluated as $B(z,a,b) = \int_0^z t^{a-1}(1-t)^{b-1}dt$

and $B(a,b)$ is the beta function [23] evaluated as $B(a,b) = \int_0^1 t^{a-1}(1-t)^{b-1}dt$.

Proof. Here, we begin by deriving the first and second moments of the numerator and the denominator of γ_L^i. Let, the numerator term be represented as $X_L = \left|\boldsymbol{h}_{i,Ric}^H \mathbf{e}_i\right|^2$ and the denominator term as $Y_L = \sum_{j\neq i}^N \left|\boldsymbol{h}_{i,Ric}^H \mathbf{e}_j\right|^2 + \frac{\beta_i^L}{P_t}\sigma^2$. Then, we have $X_L = \left|\sum_{k=1}^{M^2} \boldsymbol{h}_{i,Ric}^{k*} \boldsymbol{e}_i^k\right|^2$ where $\boldsymbol{h}_{i,Ric}^{k*} \boldsymbol{e}_i^k \sim CN\left(\sqrt{\frac{K_i}{1+K_i}}, \frac{1}{1+K_i}\right)$. Let $A_k^L := \mathrm{Re}\left(\boldsymbol{h}_{i,Ric}^{k*} \boldsymbol{e}_i^k\right)$ and $B_k^L := \mathrm{Im}\left(\boldsymbol{h}_{i,Ric}^{k*} \boldsymbol{e}_i^k\right)$. Thus, we have $X_L = \left(\sum_{k=1}^{M^2} A_k^L\right)^2 + \left(\sum_{k=1}^{M^2} B_k^L\right)^2$, where $A_k^L \sim N\left(\sqrt{\frac{K_i}{1+K_i}}, \frac{1}{2(1+K_i)}\right)$ and $B_k^L \sim N\left(0, \frac{1}{2(1+K_i)}\right)$. Thus, using the properties of normal distribution and proof of (6.1), we have

$$E(X_L) = \frac{M^4 K_i}{1+K_i} + \frac{M^2}{1+K_i}. \tag{3.1.2}$$

Similarly, we have,

$$\mathrm{Var}(X_L) = \frac{M^4}{(1+K_i)^2}\left(1 + 2K_i M^2\right). \tag{3.1.3}$$

Next, to evaluate the moments of Y_L, we note that $\boldsymbol{h}_{i,Ric}^{k*} \boldsymbol{e}_j^k \sim CN\left(\sqrt{\frac{K_i}{1+K_i}} \boldsymbol{e}_i^{k*} \boldsymbol{e}_j^k, \frac{1}{1+K_i}\right)$. Let, $C_{kj}^L := \mathrm{Re}\left(\boldsymbol{h}_{i,Ric}^{k*} \boldsymbol{e}_j^k\right)$ and $D_{kj}^L := \mathrm{Im}\left(\boldsymbol{h}_{i,Ric}^{k*} \boldsymbol{e}_j^k\right)$. Then, we have $\left|\boldsymbol{h}_{i,Ric}^H \boldsymbol{e}_j\right|^2 = \left(\sum_{k=1}^{M^2} C_{kj}^L\right)^2 + \left(\sum_{k=1}^{M^2} D_{kj}^L\right)^2$, where $C_{kj}^L \sim N\left(\mathrm{Re}\left(\mu_{ijk}\right), \frac{1}{2(1+K_i)}\right)$ and $D_{kj}^L \sim N\left(\mathrm{Im}\left(\mu_{ijk}\right), \frac{1}{2(1+K_i)}\right)$. Here, $\mu_{ijk} := \sqrt{\frac{K_i}{1+K_i}} \boldsymbol{e}_i^{k*} \boldsymbol{e}_j^k$. Again, using the properties of the normal distribution and proof of (6.1), we have $E\left(\left|\boldsymbol{h}_{i,Ric}^H \boldsymbol{e}_j\right|^2\right) = \left(\sum_{k=1}^{M^2} \mathrm{Re}\left(\mu_{ijk}\right)\right)^2 + \left(\sum_{k=1}^{M^2} \mathrm{Im}\left(\mu_{ijk}\right)\right)^2 +$

$\frac{M^2}{1+K_i}$. Thus, we have

$$E(Y_L) = \left\{ \sum_{j=1, j\neq i}^{N} \left(\sum_{k=1}^{M^2} \mathrm{Re}\left(\mu_{ijk}\right) \right)^2 + \left(\sum_{k=1}^{M^2} \mathrm{Im}\left(\mu_{ijk}\right) \right)^2 \right\} + \frac{(N-1)M^2}{1+K_i} + \frac{\beta_i^L \sigma^2}{P_t}. \tag{3.1.4}$$

$$= \frac{K_i}{1+K_i} \left\{ \sum_{j=1, j\neq i}^{N} \left(\sum_{k=1}^{M^2} \mathrm{Re}\left(\tilde{\mu}_{ijk}\right) \right)^2 + \left(\sum_{k=1}^{M^2} \mathrm{Im}\left(\tilde{\mu}_{ijk}\right) \right)^2 \right\} + \frac{(N-1)M^2}{1+K_i} + \frac{\beta_i^L \sigma^2}{P_t}, \tag{3.1.5}$$

Where, $\tilde{\mu}_{ijk} = \boldsymbol{e}_i^{k*} \boldsymbol{e}_j^k$. Similarly, neglecting the correlation of the terms in Y_L, we have

$$\mathrm{Var}(Y_L) = \frac{M^4(N-1)}{(1+K_i)^2} + \frac{2M^2 K_i}{(1+K_i)^2} \left\{ \sum_{j=1, j\neq i}^{N} \left(\sum_{k=1}^{M^2} \mathrm{Re}\left(\tilde{\mu}_{ijk}\right) \right)^2 + \left(\sum_{k=1}^{M^2} \mathrm{Im}\left(\tilde{\mu}_{ijk}\right) \right)^2 \right\}. \tag{3.1.6}$$

Next, we approximate both the numerator and the denominator as a gamma RV using the method of moment matching [24]. Thus, X_L will be approximated as a gamma RV with scale parameter and shape parameter given by

$$\theta_{L,i,1} = \frac{\mathrm{Var}[X_L]}{E[X_L]} = \frac{M^2 + 2K_i M^4}{(1+K_i)(1+K_i M^2)} \text{ and } k_{L,i,1} = \frac{\mathrm{E}[X_L]}{\theta_{L,i,1}} = \frac{(1+K_i M^2)^2}{1+2K_i M}. \tag{3.1.7}$$

$$\theta_{L,i,2} = \frac{\mathrm{Var}[Y_L]}{E[Y_L]} = \frac{2g(\boldsymbol{e}_i, \boldsymbol{e}_j)K_i M^2 + M^4(N-1)}{(1+K_i)\left(\bar{\gamma}^L + K_i(\bar{\gamma}^L + g(\boldsymbol{e}_i, \boldsymbol{e}_j))\right) + M^2(N-1)} \text{ and} \quad (3.1.8)$$

$$k_{L,i,2} = \frac{\mathrm{E}[Y_L]}{\theta_{L,i,2}} = \frac{\left(\left(\bar{\gamma}^L + K_i(\bar{\gamma}^L + g(\boldsymbol{e}_i, \boldsymbol{e}_j)\right) + M^2(N-1)\right)^2}{2g(\boldsymbol{e}_i, \boldsymbol{e}_j)K_i M^2 + M^4(N-1)}. \quad (3.1.9)$$

Where, $\bar{\gamma}^L = \frac{\beta_i^L \sigma^2}{P_t}$ and $g(\boldsymbol{e_i}, \boldsymbol{e}_j) = \sum\limits_{j=1, j\neq i}^{N} \left(\sum\limits_{k=1}^{M^2} \mathrm{Re}\left(\tilde{\mu}_{ijk}\right)\right)^2 + \left(\sum\limits_{k=1}^{M^2} \mathrm{Im}\left(\tilde{\mu}_{ijk}\right)\right)^2$.
Thus, we have $\gamma_L^i \sim \beta'\left(k_{L,i,1}, k_{L,i,2}, 1, \frac{\theta_{L,i,1}}{\theta_{L,i,2}}\right)$ and the corresponding CDF is given in (3.1.1).

□

3.2 SINR NLOS

Lemma 3.2.1. *The distribution of γ_{NL}^i can be approximated as*

$$F_{\gamma_{NL}^i}(x) = 1 - \left(1 - \frac{x}{x + \frac{\theta_{NL,i,1}}{\theta_{NL,i,2}}}\right)^{k_{NL,i,2}} \qquad \mathrm{x} > 0, \quad (3.2.1)$$

where, $\theta_{NL,i,1}$, $k_{NL,i,1}$, $\theta_{NL,i,2}$ and $k_{NL,i,2}$ can be evaluated using (3.2.2) and (3.2.3).

Proof. Note that this is a special case of the scenario considered in Lemma 3.1.1 for the case of $K_i = 0n \ \forall \ i$. Thus, following similar steps we can determine the first and second moments of the numerator and denominator of γ_{NL}^i represented as X_{NL} and Y_{NL} respectively. Again, we can use moment matching to approximate X_{NL} as

a gamma RV with scale parameter and shape parameter given by

$$\theta_{NL,i,1} = \frac{\mathrm{Var}[X_{NL}]}{E[X_{NL}]} = \frac{\vartheta_i^4}{\vartheta_i^2} = M^2 \text{ and } k_{NL,i,1} = \frac{\mathrm{E}[X_{NL}]}{\theta_{NL,i,1}} = \frac{\vartheta_i^2}{\vartheta_i^2} = 1. \tag{3.2.2}$$

Similarly, the denominator Y_{NL} can also be approximated as a Gamma RV with scale parameter and shape parameter given by

$$\theta_{NL,i,2} = \frac{\sum_{j\neq i}^{N} \vartheta_j^4}{\sum_{j\neq i}^{N} \vartheta_j^2 + \frac{\beta_i^{NL}\sigma^2}{P_t}} = \frac{(N-1)M^4}{(N-1)M^2 + \frac{\beta_i^{NL}\sigma^2}{P_t}} \text{ and } k_{NL,i,2} = \frac{(N-1)M^2 + \frac{\beta_i^{NL}\sigma^2}{P_t}}{\theta_{NL,i,2}}. \tag{3.2.3}$$

Thus, we have $\gamma_{NL}^i \sim \beta'\left(k_{NL,i,1}, k_{NL,i,2}, 1, \frac{\theta_{NL,i,1}}{\theta_{NL,i,2}}\right)$ (where, $\vartheta_i^2 = \sum_{j=1}^{M^2} |\boldsymbol{e}_i^j|^2 = M^2$.) and the corresponding CDF is given in (3.2.1).

□

Finally, approximate expressions for the distributions of the CDF of SINR LoS (γ_L^i) and the CDF of SINR NLoS (γ_{NL}^i) for i-th user are derived.

Chapter 4

Outage probability Analysis

In this chapter, we derive an expression for i-th user's Outage probability. Then, we analyze specific terms in the OP for NLoS and LoS case by varying particular system parameters.

4.1 Outage Probability expression

The outage probability of the i-th user for a threshold γ_{th} is defined as

$$OP_i = \left(P_{Los}(\theta_i^z) \times P\left(\gamma_L^i \leq \gamma_{th}\right)\right) + \left(P_{NLos}(\theta_i^z) \times P\left(\gamma_{NL}^i \leq \gamma_{th}\right)\right). \tag{4.1.1}$$

Next, we see how we can analyse the different term in OP_i with respect to the variations in certain system parameters

4.2 Analysis of OP

NLOS:

Variations with respect to N: Note that we can make the following observations from the expressions of $\theta_{NL,i,2}$ and $k_{NL,i,2}$.

$$\frac{\partial \theta_{NL,i,2}}{\partial N} = \frac{M^4 \frac{\beta_i^{NL}\sigma^2}{P_t}}{\left(M^2(N-1) + \frac{\beta_i^{NL}\sigma^2}{P_t}\right)^2} > 0, \ \forall M, \beta_i^{NL}, \sigma^2, P_t. \tag{4.2.1}$$

$$\frac{\partial k_{NL,i,2}}{\partial N} = 1 - \frac{\frac{\beta_i^{NL}\sigma^2}{P_t}}{M^4(N-1)^2} > 0, \ \forall M, \beta_i^{NL}, \sigma^2, P_t. \tag{4.2.2}$$

Using (3.2.1), the value of OP_i for the Nlos scenario can be evaluated as $1-(1-y_i)^{k_{NL,i,2}}$, where $y_i = \frac{x}{x+\frac{\theta_{NL,i,1}}{\theta_{NL,i,2}}}$. From the observations in (4.2.1) and (4.2.2), we can conclude that both $\theta_{NL,i,2}$ and $k_{NL,i,2}$ increases with an increase in the number of interferers N. This in turn would mean $(1-y_i)$ decreases and hence the outage increases.

Variations with respect to M: In this case we have,

$$\frac{\partial \theta_{NL,i,1}}{\partial M} = M > 0, \ \forall N, \beta_i^{NL}, \sigma^2, P_t. \tag{4.2.3}$$

$$\frac{\partial \theta_{NL,i,2}}{\partial M} = \frac{2(N-1)\left(M^5(N-1) + 2M^3\frac{\beta_i^{NL}\sigma^2}{P_t}\right)}{\left(M^2(N-1) + \frac{\beta_i^{NL}\sigma^2}{P_t}\right)^2} > 0, \ \forall N, \beta_i^{NL}, \sigma^2, P_t. \tag{4.2.4}$$

$$\frac{\partial k_{NL,i,2}}{\partial M} = \frac{-4\frac{\beta_i^{NL}\sigma^2}{P_t}\left(M^2(N-1) + \frac{\beta_i^{NL}\sigma^2}{P_t}\right)}{M^5(N-1)} < 0, \ \forall M, \beta_i^{NL}, \sigma^2, P_t. \tag{4.2.5}$$

Thus, from (4.2.3), (4.2.4) and (4.2.5), we can conclude that as M increases, y_i increases and $k_{NL,i,2}$ decreases, which in turn would mean that the outage decreases.

LOS:

Note that the expression for the OP in the Los scenario is more complicated and hence we cannot easily arrive at general conclusions as in the case of Nlos links. Note that $P\left(\gamma_L^i \leq \gamma_{th}\right)$ can also be evaluated as $P\left(\frac{\tilde{X}_L}{\tilde{Y}_L} \leq \frac{\gamma_{th}\theta_{L,i,2}}{\theta_{L,i,1}}\right)$ where $\tilde{X}_L \sim \text{Gamma}\left(k_{L,i,1}, 1\right)$ and $\tilde{Y}_L \sim \text{Gamma}\left(k_{L,i,2}, 1\right)$. Now, from the results in [25], we know that increasing the values of $k_{L,i,2}$ by keeping the values of $k_{L,i,1}$ and $\frac{\gamma_{th}\theta_{L,i,2}}{\theta_{L,i,1}}$ constant would increase the outage probability. Similarly, a decrease in the value of $k_{L,i,1}$ by keeping the values of $k_{L,i,2}$ and $\frac{\gamma_{th}\theta_{L,i,2}}{\theta_{L,i,1}}$ constant would also increase the outage probability. Using (3.1.7)-(3.1.9), we can evaluate the changes in the parameters of the CDF of γ_L^i and this in turn can be used to study the corresponding variations in the outage probability.

Chapter 5

Simulation Results

5.1 Simulation Setting

In this section, demonstrated the simulations to verify the results derived in the last section, and different environment parameters from Table 2.1 and Table 5.1 summarises the simulation parameters used throughout this section unless mentioned otherwise.

5.2 Simulation Results

Figure 5.1 and Fig 5.2 compare the simulated and theoretical CDF of SINR in the Los and Nlos scenarios respectively. We can observe that the simulated and the theoretical values of CDF are in good agreement for both the scenarios.

Next, in Fig 5.3 and Fig 5.4, we demonstrate the variations in the outage probability with respect to the variations in M and N. As expected, we can see that

Parameter	Value
Dimensions of the planar array M	8
UAV height z_u	50
UAV position $(x_u, y_u, -z_u)$	(0,0,0)
User's position $(x_i, y_i, -z_i)$	$(x_i, y_i, -50)$
Number of users N	2
Simulation area	Square of side L
L	30
λ	0.0128
Transmit SNR $\frac{P_t}{\sigma^2}$	1 dB

Table 5.1: Simulation Parameters

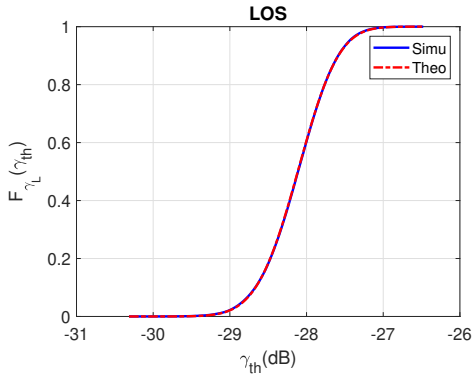

Figure 5.1: Simulated and theoretical values of the CDF of $\gamma_{L,i}$

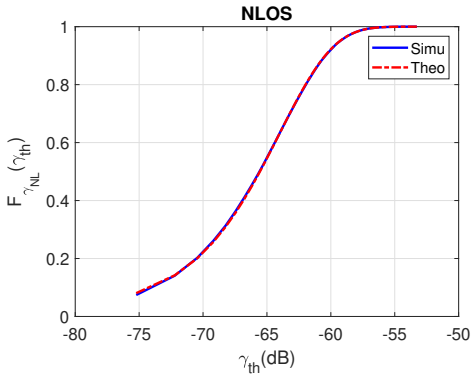

Figure 5.2: Simulated and theoretical values of the CDF of $\gamma_{NL,i}$

the outage probability decreases with an increase in the antenna array dimension and with a decrease in the number of users (which in turn reduces the number of interferers for a particular user).

5.3 Conclusions and Future Work

This proposed approach tells us that the outage probability depends on the number of users and antenna array dimension and it is demonstrated by varying the M and

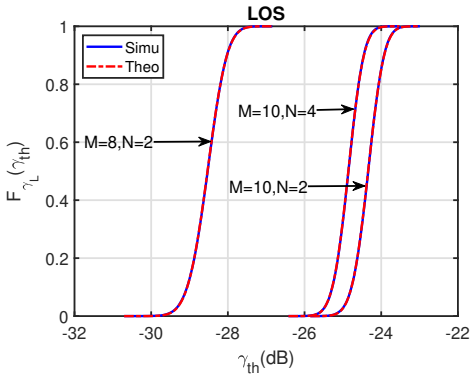

Figure 5.3: Simulated and theoretical values of the CDF of $\gamma_{L,i}$ for different values of M and N

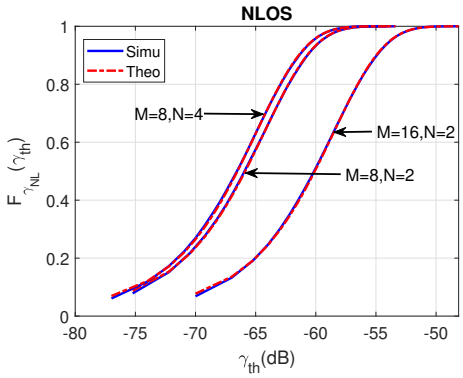

Figure 5.4: Simulated and theoretical values of the CDF of $\gamma_{NL,i}$ for different values of M and N

N for the Nlos case. For the Los case, evaluated by changing the parameters of the CDF of SINR. The UAV-aided mmWave communication is a promising candidate for the upcoming generation 5G and future mobile communication system due to its high mobility, flexibility, and sufficient bandwidth. . This work only considered that UAV is positioned at a stationary point, and in the future, it would be interesting if we do this work for Moving UAVs. Similarly, it would be more challenging and exciting to analyze UAVs when working as an emergency Base station at disaster areas, Vehicular networks, etc.

Chapter 6

Appendix

6.1 Proof of $\mathbf{e}_i^H \mathbf{e}_j$

The steering vectors e_i and e_j are given as

$$\mathbf{e_i} = \left[1, ..., e^{j\pi sin\theta_i^z\left[(m-1)cos\theta_i^a + (n-1)sin\theta_i^a\right]}, ..., e^{j\pi sin\theta_i^z\left[(M-1)cos\theta_i^a + (M-1)sin\theta_i^a\right]}\right]^T$$

$$\mathbf{e_j} = \left[1, ..., e^{j\pi sin\theta_j^z\left[(m-1)cos\theta_j^a + (n-1)sin\theta_j^a\right]}, ..., e^{j\pi sin\theta_j^z\left[(M-1)cos\theta_j^a + (M-1)sin\theta_j^a\right]}\right]^T$$

$$e_i^H . e_j = \left[1, ..., e^{-j\pi sin\theta_i^z\left[(m-1)cos\theta_i^a + (n-1)sin\theta_i^a\right]}, ..., e^{-j\pi sin\theta_i^z\left[(M-1)cos\theta_i^a + (M-1)sin\theta_i^a\right]}\right].$$

$$\left[1, ..., e^{j\pi sin\theta_j^z\left[(m-1)cos\theta_j^a + (n-1)sin\theta_j^a\right]}, ..., e^{j\pi sin\theta_j^z\left[(M-1)cos\theta_j^a + (M-1)sin\theta_j^a\right]}\right]^T$$

$$= \sum_{m=1}^{M-1} \sum_{n=1}^{M-1} e^{-j\pi sin\theta_i^z\left[(m-1)cos\theta_i^a + (n-1)sin\theta_i^a\right]} e^{j\pi sin\theta_j^z\left[(m-1)cos\theta_j^a + (n-1)sin\theta_j^a\right]}$$

$$= \sum_{m=1}^{M-1} \sum_{n=1}^{M-1} e^{-j\pi(m-1)\left[sin\theta_i^z cos\theta_i^a - sin\theta_j^z cos\theta_j^a\right]} e^{-j\pi(n-1)\left[sin\theta_i^z sin\theta_i^a - sin\theta_j^z sin\theta_j^a\right]}$$

Both summation's are independent, so divide them into individual

$$= \sum_{m=1}^{M-1} e^{-j\pi(m-1)\left[sin\theta_i^z cos\theta_i^a - sin\theta_j^z cos\theta_j^a\right]} \sum_{n=1}^{M-1} e^{-j\pi(n-1)\left[sin\theta_i^z sin\theta_i^a - sin\theta_j^z sin\theta_j^a\right]}$$

Let's take, G1 and G2 here

$$G1 = e^{-j\pi\left[sin\theta_i^z cos\theta_i^a - sin\theta_j^z cos\theta_j^a\right]}, G2 = e^{-j\pi\left[sin\theta_i^z sin\theta_i^a - sin\theta_j^z sin\theta_j^a\right]}$$

Now, substitute these variables in original equation then we get

$$e_i^H . e_j = \sum_{m=1}^{M-1} G_1^{m-1} \sum_{n=1}^{M-1} G_2^{n-1} = \sum_{m=0}^{M-1} G_1^m \sum_{n=0}^{M-1} G_2^n$$

$$= \left[\frac{1 - G_1^M}{1 - G_1}\right] \left[\frac{1 - G_2^M}{1 - G_2}\right]$$

$$= \left[\frac{1 - e^{-j\pi M\left[sin\theta_i^z cos\theta_i^a - sin\theta_j^z co\theta_j^a\right]}}{1 - e^{-j\pi\left[sin\theta_i^z cos\theta_i^a - sin\theta_j^z cos\theta_j^a\right]}}\right] \left[\frac{1 - e^{-j\pi M\left[sin\theta_i^z sin\theta_i^a - sin\theta_j^z sin\theta_j^a\right]}}{1 - e^{-j\pi\left[sin\theta_i^z sin\theta_i^a - sin\theta_j^z sin\theta_j^a\right]}}\right]$$

We can take common factors from both numerator and denominator

$$= \frac{e^{-j\pi M\left[sin\theta_i^z cos\theta_i^a - sin\theta_j^z cos\theta_j^a\right]/2}}{e^{-j\pi\left[sin\theta_i^z cos\theta_i^a - sin\theta_j^z cos\theta_j^a\right]/2}} \left[\frac{e^{j\pi M\left[sin\theta_i^z cos\theta_i^a - sin\theta_j^z cos\theta_j^a\right]/2} - e^{-j\pi M\left[sin\theta_i^z cos\theta_i^a - sin\theta_j^z cos\theta_j^a\right]/2}}{e^{j\pi\left[sin\theta_i^z cos\theta_i^a - sin\theta_j^z cos\theta_j^a\right]/2} - e^{-j\pi\left[sin\theta_i^z cos\theta_i^a - sin\theta_j^z cos\theta_j^a\right]/2}}\right]$$

$$\frac{e^{-j\pi M\left[sin\theta_i^z sin\theta_i^a - sin\theta_j^z sin\theta_j^a\right]/2}}{e^{-j\pi\left[sin\theta_i^z sin\theta_i^a - sin\theta_j^z sin\theta_j^a\right]/2}} \left[\frac{e^{j\pi M\left[sin\theta_i^z sin\theta_i^a - sin\theta_j^z sin\theta_j^a\right]/2} - e^{-j\pi M\left[sin\theta_i^z sin\theta_i^a - sin\theta_j^z sin\theta_j^a\right]/2}}{e^{j\pi\left[sin\theta_i^z sin\theta_i^a - sin\theta_j^z sin\theta_j^a\right]/2} - e^{-j\pi\left[sin\theta_i^z sin\theta_i^a - sin\theta_j^z sin\theta_j^a\right]/2}}\right]$$

Now, we can write them as Sin() function

$$= \frac{e^{-j\pi M\left[sin\theta_i^z cos\theta_i^a - sin\theta_j^z cos\theta_j^a\right]/2}}{e^{-j\pi\left[sin\theta_i^z cos\theta_i^a - sin\theta_j^z cos\theta_j^a\right]/2}} \left[\frac{sin\left(\frac{M\pi}{2}\left(sin\theta_i^z cos\theta_i^a - sin\theta_j^z cos\theta_j^a\right)\right)}{sin\left(\frac{\pi}{2}\left(sin\theta_i^z cos\theta_i^a - sin\theta_j^z cos\theta_j^a\right)\right)}\right]$$

$$\frac{e^{-j\pi M\left[sin\theta_i^z sin\theta_i^a - sin\theta_j^z sin\theta_j^a\right]/2}}{e^{-j\pi\left[sin\theta_i^z sin\theta_i^a - sin\theta_j^z sin\theta_j^a\right]/2}} \left[\frac{sin\left(\frac{N\pi}{2}\left(sin\theta_i^z sin\theta_i^a - sin\theta_j^z sin\theta_j^a\right)\right)}{sin\left(\frac{\pi}{2}\left(sin\theta_i^z sin\theta_i^a - sin\theta_j^z sin\theta_j^a\right)\right)}\right]$$

finally, lets take modulus on both sides and for i ! = j , we have $|e_i^H.e_j|$

$$= \left|\frac{sin\left(\frac{M\pi}{2}\left(sin\theta_i^z cos\theta_i^a - sin\theta_j^z cos\theta_j^a\right)\right)}{sin\left(\frac{\pi}{2}\left(sin\theta_i^z cos\theta_i^a - sin\theta_j^z cos\theta_j^a\right)\right)}\right| \left|\frac{sin\left(\frac{M\pi}{2}\left(sin\theta_i^z sin\theta_i^a - sin\theta_j^z sin\theta_j^a\right)\right)}{sin\left(\frac{\pi}{2}\left(sin\theta_i^z sin\theta_i^a - sin\theta_j^z sin\theta_j^a\right)\right)}\right|$$

For i=j , we have $|e_i^H.e_i$ |

$$= \left|\frac{sin\left(\frac{M\pi}{2}\left(sin\theta_i^z cos\theta_i^a - sin\theta_i^z cos\theta_i^a\right)\right)}{sin\left(\frac{\pi}{2}\left(sin\theta_i^z cos\theta_i^a - sin\theta_i^z cos\theta_i^a\right)\right)}\right| \left|\frac{sin\left(\frac{M\pi}{2}\left(sin\theta_i^z sin\theta_i^a - sin\theta_i^z sin\theta_i^a\right)\right)}{sin\left(\frac{\pi}{2}\left(sin\theta_i^z sin\theta_i^a - sin\theta_i^z sin\theta_i^a\right)\right)}\right|$$

Using L-Hopitals rule,we get

$$= \frac{\left(\frac{M\pi}{2}\left(sin\theta_i^z cos\theta_i^a - sin\theta_i^z cos\theta_i^a\right)\right)}{\left(\frac{\pi}{2}\left(sin\theta_i^z cos\theta_i^a - sin\theta_i^z cos\theta_i^a\right)\right)} \left|\frac{cos\left(\frac{M\pi}{2}\left(sin\theta_i^z cos\theta_i^a - sin\theta_i^z cos\theta_i^a\right)\right)}{cos\left(\frac{\pi}{2}\left(sin\theta_i^z cos\theta_i^a - sin\theta_i^z cos\theta_i^a\right)\right)}\right|$$

$$\frac{\left(\frac{M\pi}{2}\left(sin\theta_i^z sin\theta_i^a - sin\theta_i^z sin\theta_i^a\right)\right)}{\left(\frac{\pi}{2}\left(sin\theta_i^z sin\theta_i^a - sin\theta_i^z sin\theta_i^a\right)\right)} \left|\frac{cos\left(\frac{M\pi}{2}\left(sin\theta_i^z sin\theta_i^a - sin\theta_i^z sin\theta_i^a\right)\right)}{cos\left(\frac{\pi}{2}\left(sin\theta_i^z sin\theta_i^a - sin\theta_i^z sin\theta_j^a\right)\right)}\right|$$

$$= M^2$$

Bibliography

[1] W. Khawaja, I. Guvenc, D. W. Matolak, U.-C. Fiebig, and N. Schneckenburger, "A survey of air-to-ground propagation channel modeling for unmanned aerial vehicles," IEEE Communications Surveys & Tutorials, vol. 21, no. 3, pp. 2361–2391, 2019.

[2] A. Fotouhi, H. Qiang, M. Ding, M. Hassan, L. G. Giordano, A. Garcia-Rodriguez, and J. Yuan, "Survey on UAV cellular communications: Practical aspects, standardization advancements, regulation, and security challenges," IEEE Communications Surveys & Tutorials, vol. 21, no. 4, pp. 3417–3442, 2019.

[3] G. Kurt, M. G. Khoshkholgh, S. Alfattani, A. Ibrahim, T. S. Darwish, M. S. Alam, H. Yanikomeroglu, and A. Yongacoglu, "A vision and framework for the high altitude platform station (HAPS) networks of the future," arXiv preprint arXiv:2007.15088, 2020.

[4] M. Mozaffari, W. Saad, M. Bennis, and M. Debbah, "Unmanned aerial vehicle with underlaid device-to-device communications: Performance and trade-offs," IEEE Transactions on Wireless Communications, vol. 15, no. 6, pp. 3949–3963, 2016.

[5] M. M. Azari, F. Rosas, K.-C. Chen, and S. Pollin, "Ultra reliable UAV communication using altitude and cooperation diversity," IEEE Transactions on Communications, vol. 66, no. 1, pp. 330–344, 2017.

[6] V. V. Chetlur and H. S. Dhillon, "Downlink coverage analysis for a finite 3-D wireless network of unmanned aerial vehicles," IEEE Transactions on Communications, vol. 65, no. 10, pp. 4543–4558, 2017.

[7] M. M. Azari, Y. Murillo, O. Amin, F. Rosas, M.-S. Alouini, and S. Pollin, "Coverage maximization for a poisson field of drone cells," in 2017 IEEE 28th Annual International Symposium on Personal, Indoor, and Mobile Radio Communications (PIMRC). IEEE, 2017, pp. 1–6.

[8] B. Galkin, J. Kibilda, and L. A. DaSilva, "Coverage analysis for low-altitude UAV networks in urban environments," in GLOBECOM 2017-2017 IEEE Global Communications Conference. IEEE, 2017, pp. 1–6.

[9] W. Khawaja, O. Ozdemir, and I. Guvenc, "UAV air-to-ground channel characterization for mmwave systems," in 2017 IEEE 86th Vehicular Technology Conference (VTC-Fall). IEEE, 2017, pp. 1–5.

[10] M. Gapeyenko, V. Petrov, D. Moltchanov, S. Andreev, N. Himayat, and Y. Koucheryavy, "Flexible and reliable UAV-assisted backhaul operation in 5G mmWave cellular networks," IEEE Journal on Selected Areas in Communications, vol. 36, no. 11, pp. 2486–2496, 2018.

[11] J. Zhao, F. Gao, L. Kuang, Q. Wu, and W. Jia, "Channel tracking with flight control system for UAV mmWave MIMO communications," IEEE Communications Letters, vol. 22, no. 6, pp. 1224–1227, 2018.

[12] T. Cuvelier and R. W. Heath, "MmWave MU-MIMO for aerial networks," in 2018 15th International Symposium on Wireless Communication Systems (ISWCS). IEEE, 2018, pp. 1–6.

[13] S. Dutta, F. Hsieh, and F. W. Vook, "HAPS based communication using mmwave bands," in ICC 2019 - 2019 IEEE International Conference on Communications (ICC), 2019, pp. 1–6.

[14] K. Popoola, D. Grace, and T. Clarke, "Capacity and coverage analysis of high altitude platform (HAP) antenna arrays for rural vehicular broadband services," in 2020 IEEE 91st Vehicular Technology Conference (VTC2020-Spring), 2020, pp. 1–5.

[15] B. El-Jabu and R. Steele, "Cellular communications using aerial platforms," IEEE Transactions on Vehicular Technology, vol. 50, no. 3, pp. 686–700, 2001.

[16] M. R. R. Khan and V. Tuzlukov, "Null-steering beamforming for cancellation of co-channel interference in CDMA wireless communication system," in 2010 4th International Conference on Signal Processing and Communication Systems. IEEE, 2010, pp. 1–5.

[17] Y. Huo and X. Dong, "Millimeter-wave for unmanned aerial vehicles networks: Enabling multi-beam multi-stream communications," arXiv preprint arXiv:1810.06923, 2018.

[18] W. Zhong, L. Xu, Q. Zhu, X. Chen, and J. Zhou, "Mmwave beamforming for UAV communications with unstable beam pointing," China Communications, vol. 16, no. 1, pp. 37–46, 2019.

[19] W. Zhong, L. Wang, Q. Zhu, X. Chen, and J. Zhou, "Millimeter-Wave beamforming of UAV communications for small cell coverage," in Artificial Intelligence in China. Springer, 2020, pp. 281–288.

[20] L. Zhu, J. Zhang, Z. Xiao, X. Cao, D. O. Wu, and X.-G. Xia, "3-D beamforming for flexible coverage in millimeter-wave UAV communications," IEEE Wireless Communications Letters, vol. 8, no. 3, pp. 837–840, 2019.

[21] H. Vaezy, M. S. H. Abad, O. Ercetin, H. Yanikomeroglu, M. J. Omidi, and M. M. Naghsh, "Beamforming for maximal coverage in mmwave drones: A

reinforcement learning approach," IEEE Communications Letters, vol. 24, no. 5, pp. 1033–1037, 2020.

[22] H. Lei, D. Wang, K. Park, I. S. Ansari, J. Jiang, G. Pan, and M. Alouini, "Safeguarding uav iot communication systems against randomly located eavesdroppers," IEEE Internet of Things Journal, vol. 7, no. 2, pp. 1230–1244, 2020.

[23] M. Shadab, S. Jabee, and J. Choi, "An extended beta function and its applications," Far East Journal of Mathematical Sciences, vol. 103, pp. 235–251, 01 2018.

[24] S. Covo and A. Elalouf, "A novel single-gamma approximation to the sum of independent gamma variables, and a generalization to infinitely divisible distributions," Electron. J. Statist., vol. 8, no. 1, pp. 894–926, 2014. [Online]. Available: https://doi.org/10.1214/14-EJS914

[25] M. Srinivasan and S. Kalyani, "Analysis of outage probability of mrc with $\kappa-\mu$ co-channel interference," arXiv preprint arXiv:1805.07769, 2018.